PERINTIS eJournal

PERINTIS eJournal, **2020**, Vol. 10, No. 2, pp. 13-29

EFFECT OF GRAPHENE CONTENT ON THE MECHANICAL, PHYSICAL AND THERMAL PROPERTIES OF IMPACT MODIFIED POLY(LACTIC ACID) COMPOSITE

Fatin Adilah Jamsari[1], Zainoha Zakaria[1*], Muhammad Akmal Ahmad Saidi[2], Azman Hassan[2], Wong Joon Fatt[2]

[1]Department of Chemistry, Faculty of Science, Universiti Teknologi Malaysia, 81310 Johor Bahru, Malaysia
[2]School of Chemical and Energy Engineering, Faculty of Engineering, Universiti Teknologi Malaysia, 81310 Johor Bahru, Malaysia

* Corresponding author: zainoha@kimia.fs.utm.my

ABSTRACT

The objective of the study is to investigate the effect of graphene content (0.5, 1.0, 1.5 and 2.0 phr) on mechanical, physical and thermal properties of impact modified PLA. Core shell rubber (CSR) at a fixed PLA:CSR ratio (95:5) was used as the impact modifier for this study. Flexural strength and modulus were reduced with addition of CSR by 11.30% and 6.65%, respectively. However, the addition of graphene showed a fluctuated trend in the flexural strength of impact modified PLA while increasing trend was observed for the flexural modulus. PLA/CSR incorporated with 1.5 phr graphene showed the highest flexural strength at 21.6 MPa. Physical properties were analyzed through water absorption test at 30℃ and 50℃ . The incorporation of CSR and graphene decreased the water absorption at both temperatures and retarded the biodegradation of PLA. Thermal properties were analyzed using thermogravimetry analysis (TGA) and differential scanning calorimetry (DSC). TGA showed that CSR decreased the thermal stability of neat PLA by 9.1% as indicated by the initial decomposition temperature (T_5) and 7.3% for maximum decomposition temperature (T_{max}). On the other hand, the addition of graphene into PLA/CSR increased the thermal stability of the impact modified PLA. DSC analysis showed an increase in thermal stability of PLA, as indicated by the shifting of glass transition temperature (T_g) and melting temperature (T_m) to a higher temperature. Fourier Transform Infrared Spectroscopy (FTIR) was used to identify functional group and interactions in the nanocomposites. FTIR spectra showed some interaction between PLA matrix with CSR but no interaction was observed between PLA with graphene. The overall results showed the potential of graphene/CSR/PLA nanocomposite as an advanced bio-based nanocomposite.

Keywords: Graphene; poly(lactic acid); flexural test; physical properties; thermal properties

1.0 INTRODUCTION

Synthetic polymeric materials have the disadvantage of polluting the environment if their disposal are not well planned. One of the solutions to this issue is the use of biodegradable plastics such as poly(lactic acid) (PLA). PLA has caught the attention of polymer scientists as a potential biopolymer due to its good mechanical properties and suitable to be used in various applications PLA such as packaging. However, the low deformation at break and relatively high price limit its applications. To further extend its applications, several techniques have been developed to improve the properties of PLA. For instance, blending with rubbery polymers is commonly employed to improve the toughness of PLA [1]. While to control the tensile strength or degradation rate of PLA, introducing flexible chain segments through chain extension or copolymerization is found to be a good approach [2]. Besides, incorporation of nanoscale particles, such as layered silicate [3], carbon nanotubes [4] or halloysite nanotubes [5] is also an effective strategy to extend the applications of PLA because the combination of PLA with nano-structured filler is expected to produce new biodegradable and biocompatible composites with high performance or even unexpected properties.

Graphene is one of the nanofillers used to improve the properties of polymers. It is a planar monolayer of carbon atoms arranged with a carbon-carbon bond length of 0.142 nm in a two-dimensional (2D) honeycomb lattice [6]. Graphene is produced from natural graphite by micromechanical exfoliation method and is considered as a multifunctional material that can be introduced into polymers and composites. Low concentrations of graphene have been shown to improve polymer stiffness, electrical and thermal conductivity, as well as barrier properties due to its high surface area, high modulus and low density [7, 8]. The incorporation of graphene into thermoplastic polyurethane reduced about 81% of oxygen gas permeability with improved thermal conductivity about three times and mechanical strength more than five times in the study by Zahid *et al*. [7]. Meanwhile, Li *et al*. reported good electrical conductivity of graphene-reinforced epoxy nanocomposites, as well as enhanced mechanical reinforcement and thermal conductivity with only low content of graphene [8].

Core-shell rubber (CSR) is an acrylic impact modifier that has crosslinked poly(butyl acrylate) (PBA) core encapsulated in poly(methyl methacrylate) (PMMA) shell. Due to the properties of PBA and PMMA, CSR is able to improve the impact strength of polymers, such as PLA and epoxy [9-11]. In a previous study, the impact strength of PLA/multiwalled carbon nanotubes nanocomposites increased with increasing CSR content [9]. The incorporation of CSR gave better toughness for epoxy asphalt binder [10], and low content of CSR at 5 wt% is desired for its toughening effect [11]. To the best of our knowledge, no study on incorporating CSR and graphene simultaneously into PLA has been reported. Therefore, the objective of this study is to improve the mechanical and thermal properties of PLA by simultaneously incorporating graphene as a nanofiller and CSR as an impact modifier.

2.0 METHODOLOGY

2.1 Materials

PLA (Ingeo Biopolymer 3001D) in pellet form with a density of 1.24 g/cm^3 and melt flow index (MFI) of 22 g/10 min (at 210°C, 2.16 kg^{-1} loads) was obtained from NatureWorks LLC, (Minnetonka MN 55345 USA). T_g and melting temperature (T_m) of the PLA are approximately 65°C and 165°C respectively. The additives used for polymer blending in this study were CSR and graphene. The impact modifier, CSR (Paraloid EXL^{TM} 2330) was purchased from Dow Inc. (USA) in white powdered solid form with a density of 1.11 g/cm^3 and T_m of 132 to 149°C. Graphene was purchased from XG Sciences, United States of America.

2.2 Composites Preparation

All the raw materials (PLA, CSR, and graphene) were weighed according to the formulations presented in Table 1 and dried in an oven at 40°C for 24 hours to remove the moisture prior to melt blending process. The raw materials were then premixed, followed by the melt extrusion using a co-rotating twin screw extruder (Werner & Pfleiderer ZSK25, Germany). The temperature settings for compounding all of the nanocomposites were 160/175/190/200°C from the feed section to die with a rotating screw speed of 50 rpm. The extruded strand was then air-dried and pelletized. Later, the pelletized PLA nanocomposites were compression molded at 190°C by using a laboratory motor hydraulic hot press (Guthrie, Malaysia) into a 180.0 mm × 180.0 mm square plate with 2 and 3 mm thickness. The preheating, compressing, and cooling time were fixed at 2, 3 and 5 min respectively. The square plates were then cut into different dimension for sample analysis using a band saw.

Table 1 Formulation of PLA/CSR/GR nanocomposites.

Material Designation	PLA (wt%)	CSR (wt%)	Graphene (phr)
PLA	100	0	0
PLA/CSR	95	5	0
PLA/CSR/GR(0.5)	95	5	0.5
PLA/CSR/GR(1.0)	95	5	1.0
PLA/CSR/GR(1.5)	95	5	1.5
PLA/CSR/GR(2.0)	95	5	2.0

2.3 Materials Properties Characterization

2.3.1 Mechanical Properties

Flexural test was conducted using the rectangular-shaped bars (127.0 mm × 12.7 mm × 3.0 mm) of neat PLA, PLA/CSR blends and PLA/CSR/GR nanocomposites prepared from different formulations to show the effects of graphene on flexural strength and flexural modulus

at optimum filler loading. The dimensions of the specimens were carefully measured using a digital caliper. The span length was set at a span-to-depth ratio of 16. Test was carried out in laboratory atmosphere of 23℃ using universal testing machine (Zwick/Roell Z20) at test speed of 2 mm/min with a 20kN load cell.

2.3.2 Physical Properties

2.3.2.1 Water Absorption Test

Water absorption test was carried out according to ASTM D570-81. The test specimens (20.0 mm x 20.0 mm x 3.0 mm) were cut and dried at 50°C in vacuum oven until a constant weight was attained. The conditioned specimens were immersed in a container filled with water at 30°C and in a water bath at 50°C, for 14 days. Weight of specimens were recorded on daily basis. The percentage weight gain, M_t was taken as the water absorption values using Equation 1 [12]:

$$M_t, \% = [(W_i – W_o) / W_o] \times 100 \quad (1)$$

where W_o are the dry weight (before immersion) and W_i the wet weight (after immersion) of the materials, respectively.

2.3.2.2 Soil Burial Test

Soil burial test was conducted with the purpose of studying biodegradation of composites in natural conditions using garden soil, based on the method published by Thakore *et al*. [13] with slight modification. The garden soil used contained a balance of three soil materials namely silt, sand and clay with humus. It has a pH of 6 to 6.5 and high calcium levels because of its previous organic matter content. Rectangular samples (20.0 mm x 20.0 mm x 2.0 mm) were kept in a desiccator until a constant weight (W_1) was achieved. The samples were then buried in garden soil at a depth of 170 to 220 mm from the soil surface for durations of 17 weeks. The soils were sprayed with water every 24 hours to maintain their moisture. After burying at selected durations, samples were then dried at 55°C in vacuum oven and kept in desiccator until their constant weight (W_2) was achieved. The percent weight loss (% WL) was calculated according to Equation 2 [14]:

$$\% WL = [(W_1 – W_2) / W_1] \times 100 \quad (2)$$

where W_1 are the weight (before burying) and W_2 the wet weight (after burying) of the materials, respectively.

2.3.3 Thermal Properties

2.3.3.1 Thermogravimetric Analysis (TGA)

Thermogravimetric analysis (TGA) was used to investigate the thermal stability of the composite. The amount of mass loss of the PLA/CSR/GR composite when subjected to heating was determined by TGA using TGA/DSC3$^+$ Mettler Toledo Star^e system with alumina crucible using approximately 10 to 15 mg of sample. The analysis was conducted within a temperature range of 30 to 600℃ at a heating rate of 10℃/min under nitrogen atmosphere.

2.3.3.2 Differential Scanning Calorimetry (DSC)

Thermal stability of samples was determined with a TA DSC 25 (TA instruments, USA). Sample amounts ranged from 10 to 12 mg. The thermograms were recorded between 25 to 250°C at a heating rate of 1°C/min under nitrogen flow. T_g, cold crystallization temperature (T_{cc}) and T_m of the samples were determined with a TRIOS Software. The degree of crystallinity (χc) was determined as in Equation 3 [15]:

$$\chi c(\%) = \frac{\Delta H_m - \Delta H_{cc}}{\Delta H^C{}_m \, X \, \emptyset} \times 100 \quad (3)$$

where, ΔH_m is the melting enthalpy, ΔH_{cc} is the cold crystallization enthalpy, $\Delta H^C{}_m$ is the melting enthalpy of purely crystalline poly(lactic acid) and $\emptyset$ is the weight fraction of PLA in the sample.

2.3.4 Fourier Transform Infrared Spectroscopy

Attenuated Total Reflectance-Fourier Transform Infrared Spectroscopy (ATR-FTIR) was performed to characterize the chemical compositions of PLA/CSR/GR nanocomposites with different graphene content. The samples were scanned within wavenumber range of 650 to 4000 cm^{-1} using a Perkin Elmer FTIR Spectrometer Frontier. All spectra were obtained with a resolution of 8 cm^{-1} and 8 scans.

3.0 RESULTS AND DISCUSSION

3.1 Flexural Properties

The flexural strength represents the maximum stress experienced within the material before it yields in a flexural test while the flexural modulus indicates the stiffness of a material, revealing its tendency to resist bending. Flexural strength and flexural modulus of PLA and PLA/CSR blends were first compared in the Figure 1. The results showed that the effect of adding 5 wt% CSR into the PLA had caused a reduction of 14.7% and 8.17% on flexural strength and flexural modulus of the blend, respectively. The flexural strength of the blends reduced to 15.7 MPa

and its modulus decreased to 1839 MPa. This is expected due to the rubbery nature of the CSR which exhibits lower flexural properties than neat PLA. Previous study by Phattarateera and Pattamaprom [16] described that the PLA/CSR blends softened compared to neat PLA under bending force which mainly caused their properties to change. Another reason for the decreased in flexural properties of PLA/CSR composite is attributed to the lowering of crystallinity by CSR as recorded by DSC.

Figure 2 demonstrates the effect of graphene on flexural strength and flexural modulus of PLA/CSR at different content (0.5, 1.0, 1.5 and 2.0 phr). In this work, it was observed that with further addition of graphene into impact modified PLA, the flexural strength had fluctuated, which indicated that graphene gives inconsistent effect on it. Among all, PLA/CSR incorporated with 1.5 phr graphene had the highest flexural strength at 21.6 MPa. Further increase in graphene content (2.0 phr) had caused a decline on the flexural strength. The flexural strength improvement was attributed to the interaction between graphene and PLA/CSR and good dispersion of graphene inside the matrix, while decreasing flexural strength was attributed to the restacking of graphene after a certain amount due to the filler–filler attraction forces within graphene resulting in agglomeration that reduced the surface area available for stress transfer. The effect of reinforcing graphene on polymer at low content, is often associated with the polarity, molecular weight, hydrophobicity or reactive groups and other factors, which are present in the polymer and graphene [17]. Incorporation of graphene into PLA/CSR had exhibited noticeable improvement on the flexural modulus properties. These findings were consistent with previous study by Pour *et. al*. [18] who observed the flexural modulus for polycarbonate/acrylonitrile-butadiene-styrene/graphene nanoplatelets (PC/ABS/GNPs) nanocomposites was increased by 11% with the incorporation of 3 wt% GNPs. Based on their report, it is concluded that the increment of flexural modulus of PLA/CSR/GR in the present work is attributed to the interaction of the graphene with matrix when the applied stress unfolds the wavy or wrinkled structure of graphene, then provided the higher surface of interaction with matrix. Furthermore, good dispersion of the graphene in PLA/CSR matrix is one of the key factors of the improvement in this work.

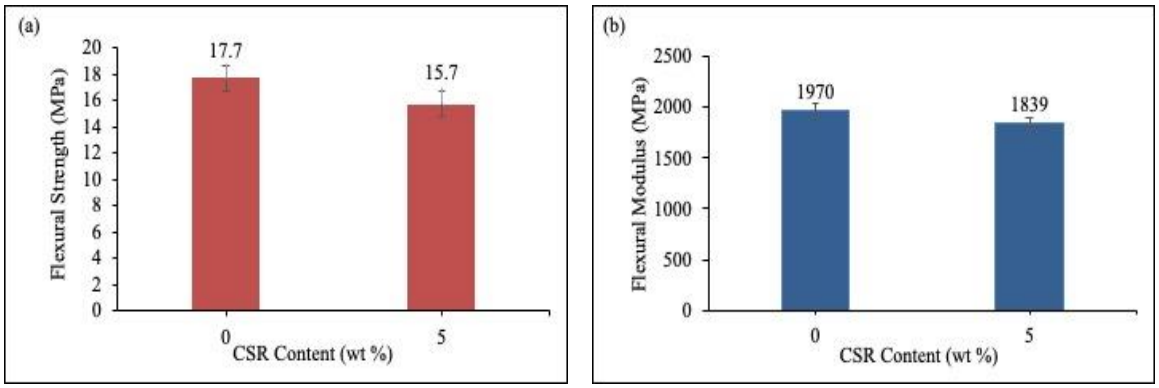

Figure 1 Effect of CSR content on (a) flexural strength and (b) flexural modulus of PLA.

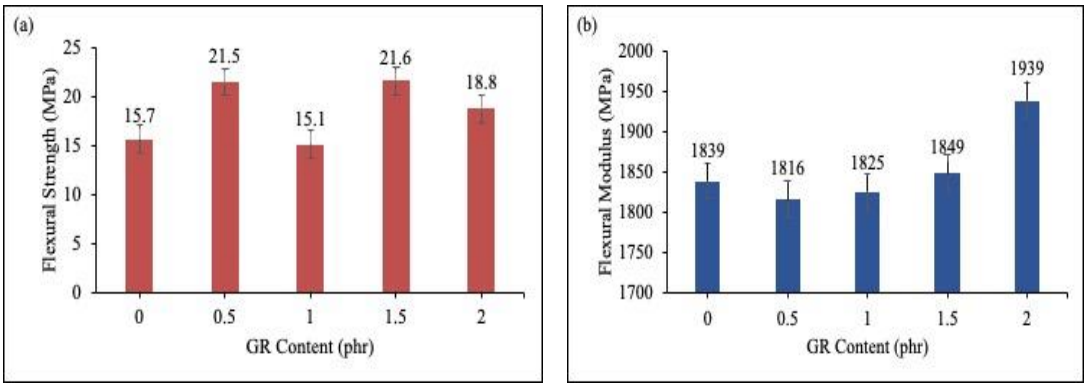

Figure 2 Effect of graphene on (a) flexural strength and (b) flexural modulus of PLA/CSR at different GR content.

3.2 Water Absorption

Table 2 summarizes the water absorption of PLA and its nanocomposites after 14 days at immersion temperature of 30℃ and 50℃. A rapid water uptake was observed for all the specimens especially within the first few days of immersion which had been attributed by hydrophilicity of PLA ester groups as shown in Figure 3 and Figure 4. The hydrolytic degradation of PLA was attributed to the attack of water molecules at ester linkages in PLA chains producing lactic acid. The formation of lactic acid oligomers from the chain scission increases the carboxylic acid end groups concentration in the medium. These carboxylic functional groups promote the degradation reaction, making the hydrolytic degradation of PLA a self-catalyzed reaction [19]. At immersion temperature of 30 ℃, the addition of CSR decreased the total water absorption of neat PLA by 0.04%, which attributed to the physical hindrance of CSR to the diffusion of water molecules. Among all PLA/CSR/GR nanocomposites, graphene content at 2.0 phr showed the highest percentage of water absorption (0.99%) but with very slight difference from those water uptakes by PLA (0.94%) and PLA/CSR (0.90%).

Table 2 Water absorption of neat PLA, PLA/CSR blend and its nanocomposites at immersion temperature of 30℃ and 50℃.

Material Designation	**Water Absorption After 2 Weeks, M_t (%)**	
	30℃	**50℃**
PLA	0.94	2.16
PLA/CSR	0.90	2.32
PLA/CSR/GR(0.5)	0.73	1.59
PLA/CSR/GR(1.0)	0.82	2.13
PLA/CSR/GR(1.5)	0.73	1.72
PLA/CSR/GR(2.0)	0.99	1.93

Figure 3 and 4 illustrate the daily water absorption of PLA and its nanocomposites at immersion temperature of 30℃ and 50℃. Water absorption test at immersion temperature of 50℃ is often referred as hygrothermal aging test. Hygrothermal aging is a degradation process which combines the effect of moisture and temperature, resulting in substantial weight loss and deterioration of mechanical properties [13]. Overall, the percentage of water uptake was significantly higher in all cases when the immersion temperature was increased to 50℃. In previous study by Balakrishnan *et. al*. [14] who observed the percentage of water uptake of PLA/montmorillonite was higher at 90℃ as compared to 60℃. According to Ishak and Berry [20], the exposure of the composite to a hot and moist environment will activate the moisture penetration (i.e, diffusion) mechanism after the occurrence of specific damage to the composites. The swellability and absorption ability of graphene which are temperature dependent could be addressed as an important factor contributing to the increasing water absorption at 50℃. In other words, high temperature increases the swelling of graphene structure, creating numbers of microvoids in PLA matrix and subsequently induces higher water absorption. At immersion temperature of 50℃, the addition of CSR had increased the water absorption of PLA by 0.16%. The acrylate rubber forming the core of CSR tends to absorb the moisture since polyacrylates are also known to be a hygroscopic material. When graphene was incorporated into PLA/CSR, the water absorption was decreased, but no clear trend is observed with increasing graphene content. It is observed that graphene at high content of 2.0 phr caused the increment of water absorption up to 0.99% at 30℃, which is attributed to the agglomeration of graphene. However, the highest water absorption at 50℃ is 2.13% by PLA/CSR with 1.0 phr graphene, and still lower than that of neat PLA and PLA/CSR blend.

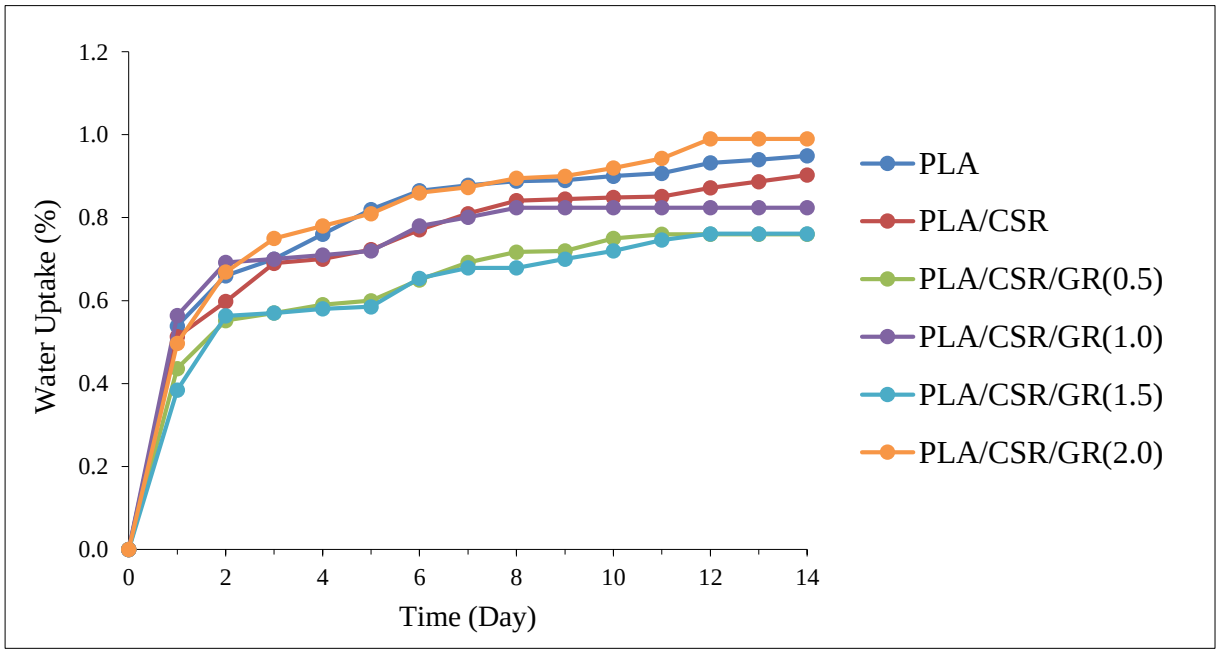

Figure 3 Water absorption of PLA and its nanocomposites at immersion temperature of 30 ℃.

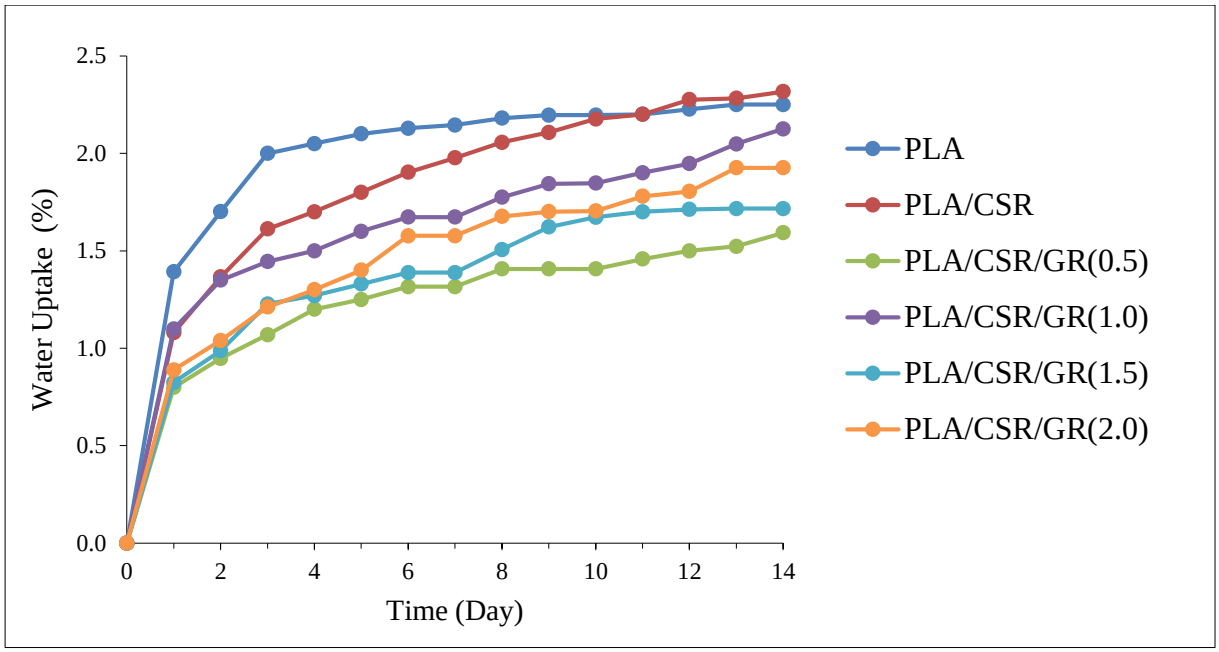

Figure 4 Water absorption of PLA and its nanocomposites at immersion temperature of 50 °C.

3.3 Biodegradability

In a soil burial test, the weight loss of a polymer is often taken to indicate the rate of degradation. Ideally, abiotic degradation takes place at the first step whereby the water molecules diffuse into the materials and attack the ester linkages in PLA molecular structure, causing the chemical hydrolysis of PLA. Next, biotic assimilation of polymer (by microorganisms) breaks down the products into water, carbon dioxide and biomass. The second step requires the presence of specific enzymes which are excreted by microorganisms such as bacteria, fungi and algae to activate the cleavage in the main chain of polyester and the residual fragments will be further utilized by the microorganisms as their source of energy [21].

From the result, it was found that pure PLA recorded a percentage of weight loss at 0.15%. This finding was similar to a previous study by Lu et. al. [22], in which pure PLA only showed 0.1% of weight loss after 24 weeks of biodegradation test. The degradation rate of PLA in soil is slow compared to other biodegradable plastics because it is only susceptible to microbial attack by certain PLA-degrading microorganisms in natural environment such as *Amycolatopsis sp.* and *Saccharotrix sp.*, in spite of its biodegradation ability [23]. It was clear that the degradation of PLA in soil was slow, subjecting to the availability of desired microorganisms and may take a long time for degradation to start in some conditions. Referring to Table 3, a slight decrease of 0.04% in the percentage of weight loss was observed when CSR was incorporated into neat PLA. This phenomenon could be explained by the high molecular

weight and crosslinks of CSR which physically retarded the degradation rate of PLA. However, the rate of degradation was further decreased after graphene was incorporated into PLA/CSR in different content. It can be observed that the presence of CSR and graphene had retarded the biodegradation of PLA.

Table 3 Percentage of weight loss of PLA, PLA/CSR blend and its nanocomposites after soil burial test of 17 weeks.

Material Designation	Weight Loss, WL (%)
PLA	0.15
PLA/CSR	0.11
PLA/CSR/GR(0.5)	0.08
PLA/CSR/GR(1.0)	0.07
PLA/CSR/GR(1.5)	0.09
PLA/CSR/GR(2.0)	0.08

3.4 Thermogravimetry Analysis (TGA)

In this work, single-stage decomposition was carried which neat PLA and its nanocomposites were analyzed under nitrogen atmosphere. The detail variation on the degradation temperature and the residual weight at 600°C for neat PLA and its nanocomposites are summarized in Table 4. Based on TGA result, it was noticed that the neat PLA possessed an initial decomposition temperature (T_5) at 309.8°C and maximum decomposition temperature (T_{max}) at 358.6°C. The decomposition of PLA at mass loss of 5% was related to the random chain scission of PLA backbone chains, as reported by Tham et. al. [24]. Addition of CSR had caused the $T_{5\%}$ and T_{max} of neat PLA to be reduced to 281.7°C and 332.3°C respectively.

Table 4 TGA results for PLA, PLA/CSR blend and its nanocomposites.

Material Designation	T_5 (°C)	T_{max} (°C)	Residual Weight at 600 °C (%)
PLA	309.8	358.6	0.00
PLA/CSR	281.7	332.3	0.70
PLA/CSR/GR(0.5)	299.2	335.2	0.79
PLA/CSR/GR(2.0)	290.6	339.5	1.82

Figure 5 shows (a) the effect of CSR on thermal stability of PLA and (b) the effect of graphene content on thermal stability of PLA/CSR. After incorporation of graphene, $T_{5\%}$ of the PLA/CSR/GR nanocomposites (Figure 5 (b)) shows a shifting to a higher temperature as compared with PLA/CSR blend. However, the inclination still could not pass the higher value of thermal decomposition that the neat PLA possessed. The only possible reason for this outcome was mainly due to the presence of CSR in the PLA/CSR/GR (0.5) which lowered the thermal stability of the nanocomposite, and weaken the effect of graphene that incorporated into the system. Further addition of graphene to 2.0 phr led to a shifting of thermal decomposition temperature to a lower temperature as shown in Table 4 for both T_5 and T_{max}. This indicates that agglomeration of graphene might have disrupted the properties of nanofillers.

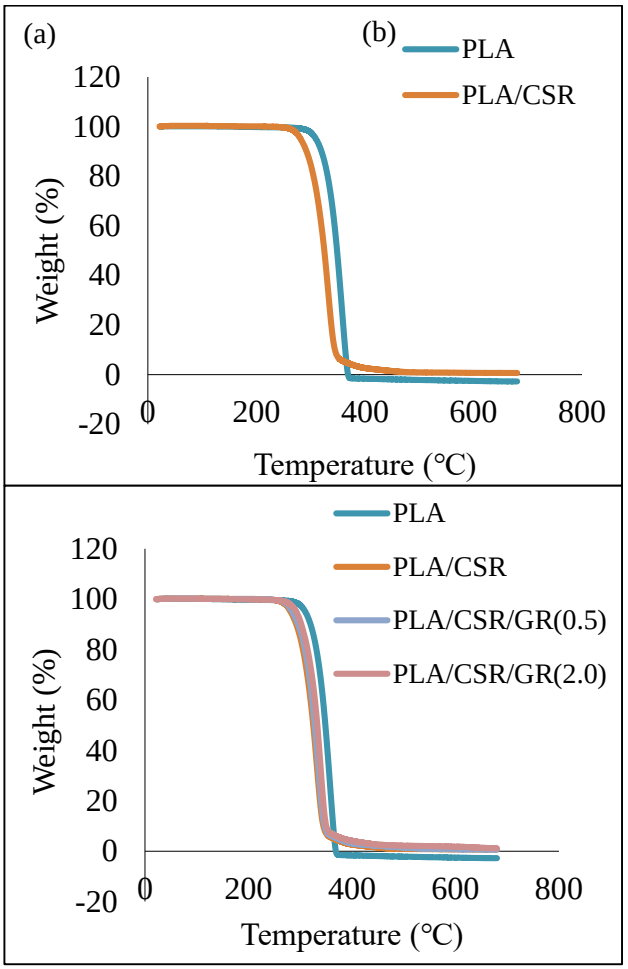

Figure 5 (a) Effect of CSR on thermal stability of PLA and (b) effect of graphene content on thermal stability of PLA/CSR.

3.5 Differential Scanning Calorimetry (DSC)

DSC thermograms of PLA and its nanocomposites are shown in Figure 6 and their thermal characteristics are summarized in Table 5. Table 5 presents T_g, T_m, T_{cc}, and χ_c obtained from the DSC analysis for neat PLA and its nanocomposites. It was interesting to note that the crystallization temperature peak for PLA did not appear during cooling in both PLA and PLA/CSR nanocomposites. It was believed that the main reason for this occurrence was due to a very slow crystallization rate of PLA during cooling [25].

T_g is defined as the temperature below which a polymer is hard and brittle (glass state) and above which is soft and flexible (rubbery state), which occurs only in amorphous regions of a polymer. Based on Table 5, the neat PLA demonstrates T_g at 57.2°C. The addition of CSR at 5 wt % had slightly increased T_g by 2.1% to 58.4°C, which shows similar observation to the study reported by Phattarateera and Pattamaprom [16]. The crystallization temperature of PLA was increased significantly from 76.4 to 96.7°C when CSR was added. It was suggested that the addition of impact modifier decreases the ability of PLA to crystallize. Moreover, T_m of PLA/CSR makes no noticeable change to those of neat PLA. In this study, PLA/CSR possessed lower χ_c than that of neat PLA. It is known that CSR basically consists of PBA and PMMA, it might have inhibited nucleation crystallization of PLA, as these molecules contained in CSR existed as melt state between the temperatures associated with cold crystallization of PLA [26]. In addition, incorporation of graphene at different content (0.5, 1.0, 1.5 and 2.0 phr) shows no appreciable changes in the T_g and T_m of PLA/CSR but T_g is still higher as compared to neat PLA. The result of T_{cc} shows fluctuated trend as well after incorporation of different graphene content. Surprisingly, only slight improvement is observed for χ_c of PLA/CSR/GR nanocomposite with 1.0 phr graphene, which requires future investigation.

Table 5 Thermal characteristics of PLA, PLA/CSR blend and its nanocomposites recorded from DSC thermograms.

Sample Designation	**T_g (°C)**	**T_m (°C)**	**T_{cc} (°C)**	**χ_c (%)**
PLA	57.2	167.7	76.4	46.68
PLA/CSR	58.4	167.8	96.7	23.56
PLA/CSR/GR(0.5)	60.5	167.4	99.6	20.36
PLA/CSR/GR(1.0)	59.1	167.3	97.9	23.92
PLA/CSR/GR(1.5)	59.4	168.1	108.1	10.78
PLA/CSR/GR(2.0)	59.0	167.5	99.4	18.98

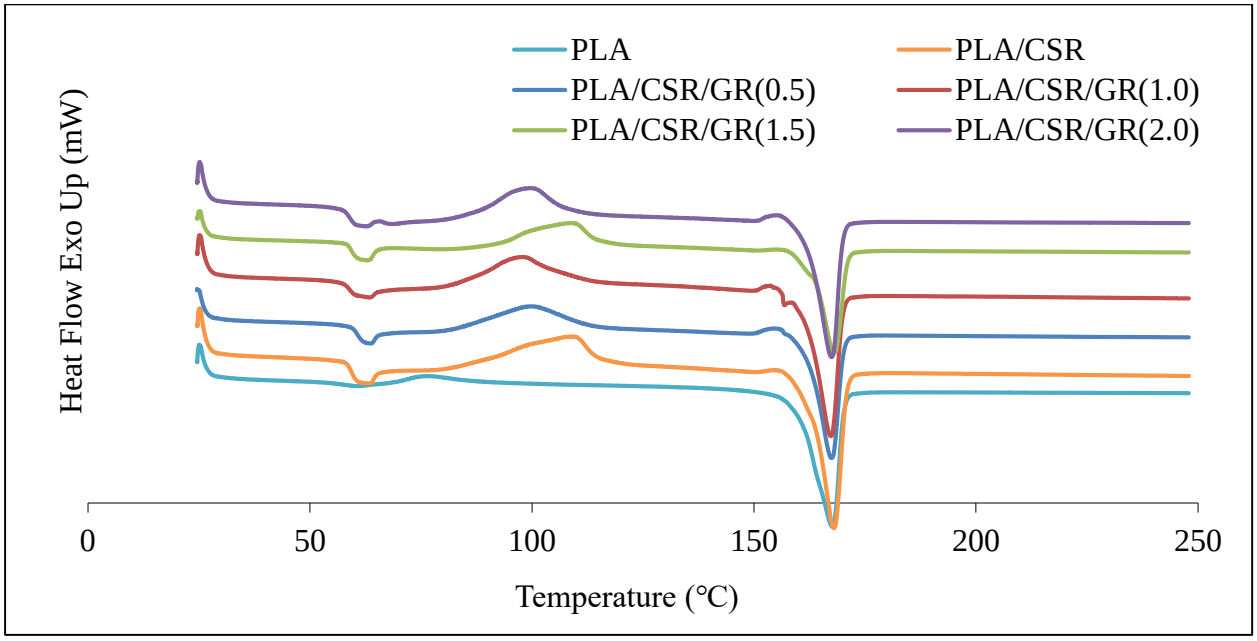

Figure 6 DSC thermograms of PLA, PLA/CSR blend and its nanocomposites.

3.6 Fourier Transform Infrared Spectroscopy Analysis

The spectrum in Figure 7 exhibits CH_3 stretching (2900 to 3000 cm^{-1}) and bending (~1450 cm^{-1}) regions in all formulations which presumably represent the CH_3 bonding of the PLA. Also, in all formulations, a sharp C=O stretching peak present at ~1750 cm^{-1} and C-O-C stretching peak at 1180 to 1080 cm^{-1} characterize the present of ester bonds in PLA. The O-H bond of PLA was present at ~3400 cm^{-1} region but at lower intensity. These results presumably due to low amount of terminal hydroxyl group present at the surface of the PLA. The characteristic peak of the graphene was not be obvious as shown in Figure 7 when graphene is incorporated into PLA/CSR blends.

Interestingly, the FTIR spectra of PLA/CSR blend show the absence of O-H bond which indicates the occurrence of interaction between PLA and CSR. It is interesting to note that CSR has a unique core and shell structure, where the core was crosslinked PBA rubber encapsulated in PMMA shell. Hence it was deduced that the PMMA shell of CSR was responsible for the observed interaction with PLA. The possible interaction between PMMA and PLA might occur through dipolar interaction between the ester groups of both polymers' phases. The highly electronegative oxygen atom in the carboxyl group of both PLA and PMMA pulls electron density away from the nearby carbon atom. Therefore, the oxygen atom carries excessive electron which made them partially negative charge, while the less electron density carbon atom possesses partially positive charge. Therefore, the difference polarity exhibited by the ester groups leads to dipolar interaction between PLA and the PMMA shell of CSR. The possible dipole interaction between PLA and PMMA was also suggested by Zhang et. al. [17].

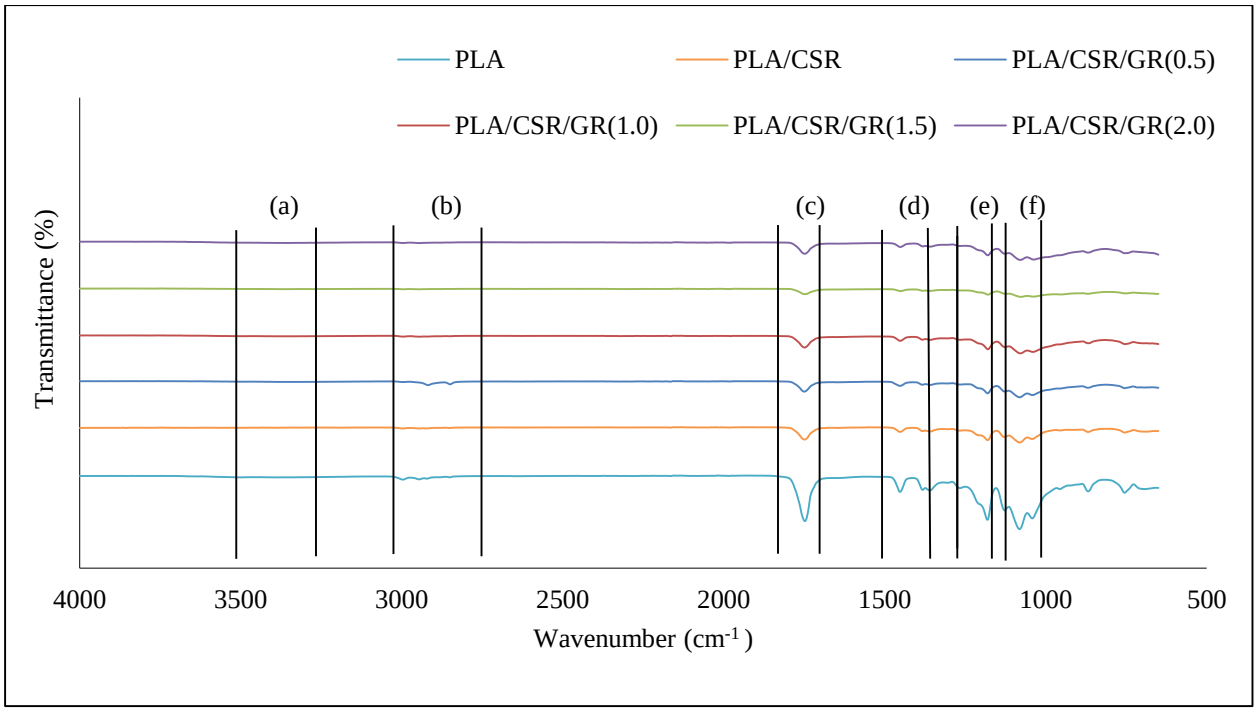

Figure 7 FTIR spectra of neat PLA, PLA/CSR blend and its nanocomposites; (a) O-H stretching (b) CH_3 stretching (c) C=O stretching (d) C-H bending (e) O-H bending (f) C-O-C stretching.

4.0 CONCLUSIONS

In this study, the effects of graphene on mechanical, physical and thermal properties of impact modified PLA were investigated. FTIR spectra showed some interaction between PLA matrix with CSR but no appreciable interaction was observed between graphene and PLA. The incorporation of 5 wt% CSR into the PLA had decreased both flexural strength and modulus of the PLA/CSR samples. No obvious trend was observed for flexural strength when different graphene content was incorporated in PLA/CSR/graphene nanocomposites while the flexural modulus showed an increase with increasing graphene content. Besides, the incorporation of CSR and graphene had decreased the water uptake and biodegradation rate of PLA. It was also observed from water absorption study that the water uptake of all samples were higher at 50℃ compared to 30℃. Thermal analysis done by TGA showed that CSR lowered the thermal stability of neat PLA. However, the addition of graphene into PLA/CSR improved the thermal stability of the impact modified PLA. DSC also showed an improvement in thermal stability of PLA with the incorporation of PLA as indicated by shifting T_g and T_m to a higher temperature. The overall results showed the potential of graphene/CSR/PLA nanocomposites as an advanced bio-based nanocomposite.

Acknowledgement

The authors would like to express their appreciation to Faculty of Science and Faculty of Engineering, Universiti Teknologi Malaysia for providing the facilities and equipment.

REFERENCES

[1] Sarazin, P., Li, G., Orts, W., & Favis, B. (2008). Binary and ternary blends of polylactide, polycaprolactone and thermoplastic starch. *Polymer*, 49(2), 599-609.

[2] Huang, C., Tsai, S., & Chen, C. (2006). Isothermal crystallization behavior of poly(L-lactide) in poly(L-lactide)-block-poly(ethylene glycol) diblock copolymers. *Journal of Polymer Science Part B: Polymer Physics*, 44(17), 2438-2448.

[3] Wu, D., Wu, L., Wu, L., Xu, B., Zhang, Y., & Zhang, M. (2008). Comparison between isothermal cold and melt crystallization of polylactide/clay nanocomposites. *Journal of Nanoscience and Nanotechnology*, 8(4), 1658-1668.

[4] Wu, D., Wu, L., Zhou, W., Zhang, M., & Yang, T. (2010). Crystallization and biodegradation of polylactide/carbon nanotube composites. *Polymer Engineering & Science*, 50(9), 1721-1733.

[5] Ang, H. T., Zakaria, Z., Ahmad Saidi, M. A., & Hassan, A. (2020). Effect of halloysite nanotubes on the mechanical, physical and thermal properties of impact modified poly(lactic acid). *PERINTIS eJournal*, 10(1), 50-68.

[6] Galpaya, D., Wang, M., Liu, M., Motta, N., Waclawik, E., & Yan, C. (2012). Recent advances in fabrication and characterization of graphene polymer nanocomposites. *Graphene*, 1(2), 30-49.

[7] Zahid, M., Del Río Castillo, A., Thorat, S., Panda, J. K., Bonaccorso, F., & Athanassiou, A. (2020). Graphene morphology effect on the gas barrier, mechanical and thermal properties of thermoplastic polyurethane. *Composites Science and Technology*, 200, 108461.

[8] Li, Y., Zhang, H., Porwal, H., Huang, Z., Bilotti, E., & Peijs, T. (2017). Mechanical, electrical and thermal properties of *in-situ* exfoliated graphene/epoxy nanocomposites. *Composites Part A: Applied Science and Manufacturing*, 95, 229-236.

[9] Mat Desa, M., Hassan, A., Arsad, A., & Arjmandi, R. (2019). Effect of core-shell rubber toughening on mechanical, thermal, and morphological properties of poly(lactic acid)/multiwalled carbon nanotubes nanocomposites. *Journal of Applied Polymer Science*, 136(28), 47756.

[10] Su, W., Han, X., Xi, Z., Zhang, J., Wang, Q., & Xie, H. (2020). Toughening epoxy asphalt binder using core-shell rubber nanoparticles. *Construction and Building Materials*, 258, 119716.

[11] Tsang, W. L., & Taylor, A. C. (2019). Fracture and toughening mechanisms of silica-core-shell rubber-toughened epoxy at ambient and low temperature. *Journal of Materials Science*, 54, 13938-13958.

[12] Chow, W., Abu Bakar, A., & Mohd Ishak, Z. (2005). Water absorption and hygrothermal aging study on organomontmorillonite reinforced polyamide 6/polypropylene nanocomposites. *Journal of Applied Polymer Science*, 98(2), 780-790.

[13] Thakore, I., Desai, S., Sarawade, B., & Devi, S. (2001). Studies on biodegradability, morphology and thermo-mechanical properties of LDPE/modified starch blends. *European Polymer Journal*, 37(1), 151-160.

[14] Balakrishnan, H., Hassan, A., Imran, M., & Wahit, M. U. (2011). Aging of toughened polylactic acid nanocomposites: water absorption, hygrothermal degradation and soil burial analysis. *Journal of Polymers and the Environment*, 19(4), 863-875.

[15] Valapa, R., Pugazhenthi, G., & Katiyar, V. (2015). Effect of graphene content on the properties of poly(lactic acid) nanocomposites. *RSC Advances*, 5(36), 28410-28423.

[16] Phattarateera, S., & Pattamaprom, C. (2019). Comparative performance of functional rubbers on toughness and thermal property improvement of polylactic acid. *Materials Today Communications*, 1(19), 374-382.

[17] Zhang, H., Zheng, W., Yan, Q., Yang, Y., Wang, J., Lu, Z., Ji, G., & Yu, Z. (2010). Electrically conductive polyethylene terephthalate/graphene nanocomposites prepared by melt compounding. *Polymer*, 51(5), 1191-1196.

[18] Pour, R., Hassan, A., Soheilmoghaddam, M., & Bidsorkhi, H. (2014). Mechanical, thermal, and morphological properties of graphene reinforced polycarbonate/acrylonitrile butadiene styrene nanocomposites. *Polymer Composites*, 37(6), 1633-1640.

[19] Tsuji, H., & Ikada, Y. (2000). Properties and morphology of poly(L-lactide). *Polymer Degradation & Stability*, 67, 179-189.

[20] Ishak, Z.M. & Berry, J. (1994). Hygrothermal aging studies of short carbon fiber reinforced nylon 6. *Journal of Applied Polymer Science*, 51(13), 2145-2155.

[21] Karamanlioglu, M. & Robson, G.D. (2013). The influence of biotic and abiotic factors on the rate of degradation of poly (lactic) acid (PLA) coupons buried in compost and soil. *Polymer Degradation & Stability*, 98(10), 2063-2071.

[22] Lu, H., Madbouly, S. A., Schrader, J. A., Srinivasan, G., McCabe, K. G., Grewell, D., & Graves, W. R. (2014). Biodegradation behavior of poly (lactic acid)(PLA)/distiller's dried grains with solubles (DDGS) composites. *ACS Sustainable Chemistry & Engineering*, 2(12), 2699-2706.

[23] Jarerat, A., & Tokiwa, Y. (2003). Poly (L-lactide) degradation by *Saccharothrix waywayandensis*. *Biotechnology letters*, 25(5), 401-404.

[24] Tham, W. L., Poh, B. T., Ishak, Z. A. M., & Chow, W. S. (2014). Thermal behaviors and mechanical properties of halloysite nanotube-reinforced poly (lactic acid) nanocomposites. *Journal of Thermal Analysis and Calorimetry*, 118(3), 1639-1647.

[25] Balakrishnan, H., Hassan, A., & Wahit, M. (2010). Mechanical, thermal, and morphological properties of polylactic acid/linear low density polyethylene blends. *Journal of Elastomers & Plastics*, 42(3), 223-239.

[26] Yeh, J. T., Tsou, C. H., Huang, C. Y., Chen, K. N., Wu, C. S., & Chai, W. L. (2010). Compatible and crystallization properties of poly(lactic acid)/poly(butylene adipate-co-terephthalate) blends. *Journal of Applied Polymer Science*, 116(2), 680-687.